Dynamic Analysis of a CubeSat launch

Geise A. Pereira[1], Reyolando M. L. R. F. Brasil[2]

[1]*Dept. of Structural and Geotechnic Engineering, University of São Paulo*
Av. Prof. Almeida Prado, building 2 n.º 83, 05508-900, São Paulo, Brazil
geise.pereira@usp.br
[2]*Dept. of Structural and Geotechnic Engineering, University of São Paulo*
Av. Prof. Almeida Prado, building 2 n.º 83, 05508-900, São Paulo, Brazil
reyolando.brasil@usp.br

Abstract. Dynamic analysis is essential in the initial design phase of a CubSat because it identifies the natural vibration frequencies, possible deformations and stresses induced by vibrations, and resonance that may occur due to the vibrations of the rocket at the time of its launch. Aiming at safety and mitigation of structural failures based on the CubeSat Design specifications and the system requirements of the QB50 project, this work evaluates the launch of a CubeSat – 1U with dimensions of 0.10m x 0.10m x 0.10m through terms of modal analysis, harmonic response, random vibrations and specific software with the objective of evaluating, through numerical analysis, the launch conditions of this kind of nanosatellite.

Keywords: CubeSat, Undamped free vibrations, Dynamics analysis, satellite launching.

1. Introduction

According to Furger [01], CubeSats are a class of nanosatellites that follow guidelines established by California State Polytechnic University, San Luis Obispo Cal Poly [02], with the goal of reducing costs and development time, increasing space accessibility consciously, and supporting frequent launches for missions aimed at conducting various experiments such as Earth mapping: special climate monitoring, deforestation control, forest fires, maritime traffic, oil spills in oceans, urban growth, precision agriculture, mining, development of new spacecraft components/architecture, among other applications.

CubeSats are a class of nanosatellites developed to reduce mission cost and development time. According to Furger [01], they follow guidelines from Cal Poly [02], allowing modular design (1U, 2U, 3U, etc.) with maximum mass per unit of 1.33 kg. These satellites support missions involving Earth observation, climate monitoring, maritime surveillance, and space technology validation.

Rivera [04] cites that CubeSats are safely stored by an orbital deployer that also has the function of ejecting the CubeSat at the right time. These deployers face a launch environment with random vibrations and shocks with high loads that can cause failures during launch Barsoum et al. [11].

Compatibility between the two according to the design specifications is one of the main requirements to ensure a perfect fit and, consequently, achieve mission success.

This paper presents the dynamic analysis of a CubeSat unit considering the structural vibration behavior during launch, using ANSYS®. The objective was to perform the dynamic analysis and detail the CubeSat model in its launch environment by performing a numerical simulation based on the solid finite element method. The mass-spring-damper model for a multiple degrees of freedom oscillator was analyzed, including the presence of a linear viscous damper for energy dissipation in structural engineering problems (friction in the

connections, air resistance and internal dissipation due to inelastic effects) as suggested by Mazzilli et al. [05].

The vibration frequencies of these modes will be determined and compared with the proposed limits for the steady-state launch excitation frequency. The effects of gravity, bending moments, and normal stresses on the structural parts under consideration will be compared with the allowable stress of the material.

2. Mathematical model and numerical parameters

The simplified model (Figure 01) considers a rigid CubeSat 1U structure (mass m = 1.33 kg) made of 6061-T6 aluminum alloy (elastic modulus E = 69 GPa, density $\rho = 2700$ kg/m³, Poisson's ratio $\nu = 0.3$, thickness = 1.5 mm). Damping was included with a ratio of $\xi = 2\%$, simulating realistic energy dissipation during launch conditions.

According to Barsoum et al. [11] 6061-T6 aluminum was chosen for the CubeSat's primary and secondary structures because it offers excellent adhesion characteristics, good acceptance of applied coatings, workability, and high structural and corrosion resistance. The simplified model considered the simulation of a CubeSat unit coupled to a P-POD orbital launcher developed by California Polytechnic State University, with the boundary condition of partial fixation of three rail slots to simulate contact with the launcher. The support condition was “limited slip” to allow some vibrational freedom with damping $\xi = 0{,}02$ in vibration modes.

Similar to the research by Barsoum et al. [11], this research also suggests the same material for the CubeSat structure to provide excellent adhesion characteristics, good economy of the applied coatings, workability, and high structural and corrosion resistance. The simplified model currently simulates a CubeSat unit attached to a P-POD orbital launcher, with a partial attachment boundary condition of three rail humps to simulate contact with the launcher.

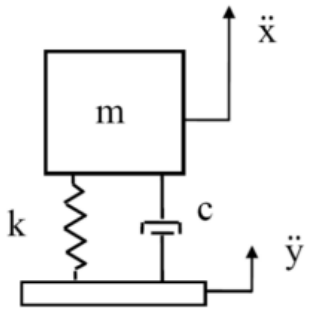


Figure 01: Mathematical model (mass-spring-damper system)

3. Modal analysis

The system can be better represented by second-order ordinary differential trading as per Eq. 01, according to Brasil and Silva [07] based on Newton's Second Law:

$$M\ddot{U} + C\dot{U} + KU = P(t) \tag{01}$$

where

M,C,K,U, $\dot{U}$, $\ddot{U}$ and P(t) are respectively, mass matrix, viscous damping matrix, stiffness matrix, displacement vector, velocity vector, acceleration vector and external forces matrix.

According to Furger [01] given a velocity and an initial input, this innovation can be resolved into the temporal response of the free vibration, which results in a simple harmonic motion that decays at an exponential rate.

The oscillation that occurs in free vibration generates the natural frequency of a System that, disregarding the first-order damping term, can be obtained from Eq. 01 and is shown in Eq. 02:

$$\omega_n = \sqrt{k/m} \tag{02}$$

The presence of damping in the system generates an exponential reduction during free vibration, with significantly high values reducing the amplitude of the oscillation at a much faster rate. The damping ratio (Eq. 03) should be defined as the damping in a system divided by the damping ratio that would critically damp the entire system (Ccr), as shown in (Eq. 04).

$$\xi = C/C\text{cr} \tag{03}$$

$$C_{\text{cr}} = 2\text{m}\ \omega_{\text{n}} = 2\sqrt{km} \tag{04}$$

When damping is added, it directly impacts the natural frequency of the entire system; as it increases, the natural frequency decreases. The damped natural frequency (d) can be calculated using Eq. 05:

$$\omega_{\text{d}} = \omega_{\text{n}}\sqrt{1-\xi^2} \tag{05}$$

4. Finite Element Methods

The finite element structural analysis process replaces the continuous mathematical model by dividing the problem domain into small but finite-dimensional subdomains, joined at points called nodes, according to Yserentant [14]. Approximately 20,000 small mesh units (SOLID186, 20-node hexagonal) were considered in the finite element analysis, each 2 mm in size, with automatic refinement at the edges using ANSYS® Mechanical software, version 2023 R2 (with a modal convergence draw with an error <0.5%).

Obtaining the equations of motion for the geometric subdomains first allows for the subsequent construction of a system of equations of motion for the mesh. According to Martha [13], the parameters of the equations of motion for finite elements should be obtained through the principles of virtual displacements, as shown in Eqs. 06 to 09:

$$\mathrm{M}_{\mathrm{L}}^{(\mathrm{e})} = \int_{\mathrm{V_e}} \mathrm{N}^{\mathrm{T}} \rho\ \mathrm{N}\ \mathrm{dV_e} \tag{06}$$

$$\mathrm{C}_{\mathrm{L}}^{(\mathrm{e})} = \int_{\mathrm{V_e}} \mathrm{N}^{\mathrm{T}} \mathrm{c}\ \mathrm{N}\ \mathrm{dV_e} \tag{07}$$

$$\mathrm{K}_{\mathrm{L}}^{(\mathrm{e})} = \int_{\mathrm{V_e}} \mathrm{B}^{\mathrm{T}}\ \mathrm{EB}\ \mathrm{dV_e} \tag{08}$$

$$\mathrm{f}_{\mathrm{L}}^{(\mathrm{e})}(\mathrm{t}) = \int_{\mathrm{V_e}} \mathrm{N}^{\mathrm{T}} \mathrm{p}(\mathrm{t})\ \mathrm{dV_e} + \int_{\mathrm{S_e}} \mathrm{N}^{\mathrm{T}} \mathrm{q}(\mathrm{t})\ \mathrm{dS_e} \tag{09}$$

where

N, L, p(t), q(t), ρ, c, V_e, and S_e are, respectively, the matrix of interpolation functions, the matrix of differential operators, the components of the volume forces, the components of the surface forces, the mass per unit volume, the viscous damping coefficient, the element volume, and the element area.

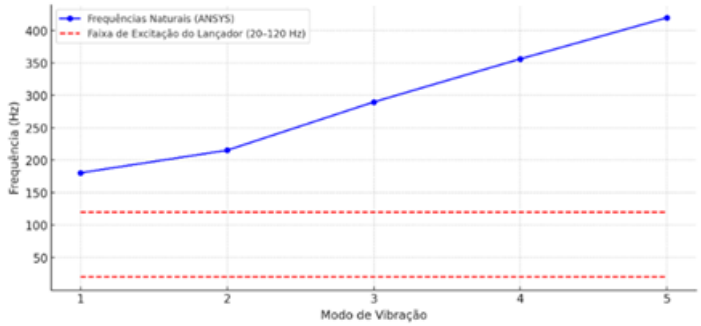
5. Results and discussions

The evaluation of the static response of the structure is performed using the ANSYS® Finite Element software where the first five natural vibration frequencies of the CubeSat were obtained according to table 01. The excitation frequency of the launch of a CubeSat by the P-POD orbital launcher is found in several scientific productions with a value of 20 Hz to 120 Hz.

Mode	Frequency (Hz)
1	180,5
2	215,3
3	289,7
4	356,2
5	419,8

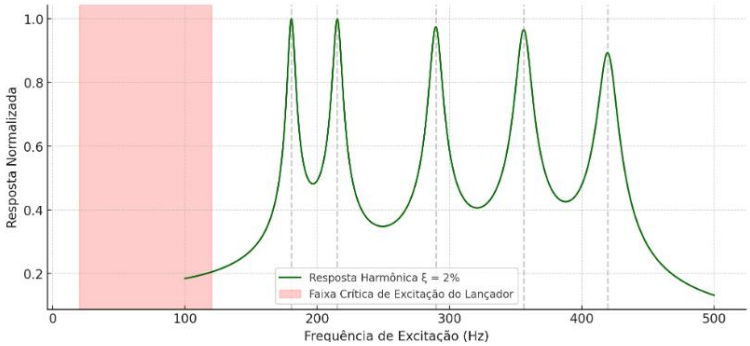
Table 01: Natural vibration frequencies x vibration modes

The first vibration mode, at a frequency of 180.5 Hz, is higher than the launcher's excitation frequency, reducing the risk of structural resonance. This is best seen in Figure 1, which shows the typical range of excitation induced by launchers during launch. Solid finite element modeling provided robust results consistent with the literature, demonstrating the applicability of the method to structural designs of small satellites.



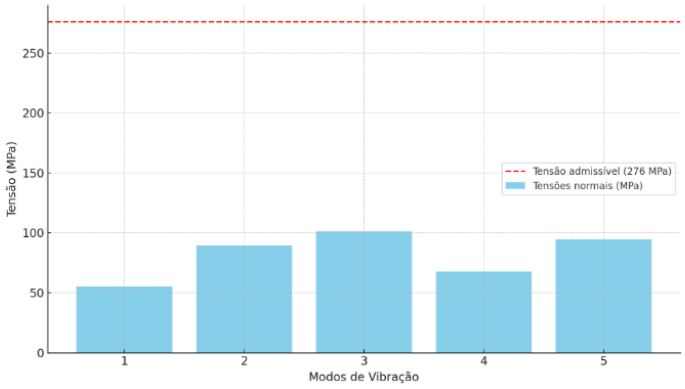
Graph 01: Natural frequencies vs. excitation frequencies of the P-POD orbital launcher (ANSYS®).

Graph 02 presents different external harmonic responses (generated by the rocket) considering a damping factor of $\xi = 2\%$ (green line), the natural frequencies of the first five modes (gray lines) and the critical excitation region of the P-POD orbital launcher during launch (pink band).



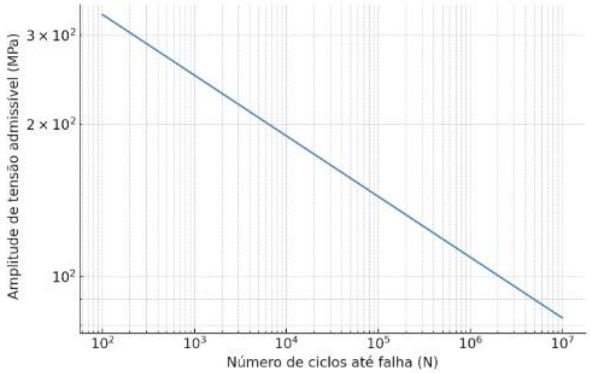
Graph 02 – Harmonic response spectrum including natural frequencies (gray), damping ($\xi = 2\%$), and launcher excitation band (red).

The maximum normal stresses obtained in the first five vibration modes (blue bars) vary between 55 MPa and 101 MPa and are compared with the allowable stress of 6061-T6 aluminum (dashed red line) and are better presented in graph 03:



Graph 03: Allowable material stress x normal stresses (ANSYS®).

The fatigue assessment of 6061-T6 aluminum can be seen in Graph 4, which shows the relationship between the number of loading cycles and the withstand stress amplitude before fatigue failure. For approximately 10 cycles (typical of a launch with random vibratory loads), the structure supports a stress amplitude of around 150 MPa. If stresses during launch are below this limit (which is common with design margins), the risk of fatigue failure is low.



Graph 04: Fatigue assessment (ANSYS®).

6. Conclusions

Based on detailed structural modeling performed using the solid finite element method in ANSYS® software, it was possible to evaluate the first five vibration modes, normal stress levels, global resonance risks, and fatigue limits for a 1U CubeSat unit manufactured in 6061-T6 aluminum alloy.

Modal analysis performed in the software allowed us to identify the natural frequencies and principal mode shapes to evaluate the dynamic performance of CubeSats and prevent the structure's natural frequencies from being amplified by the vibration levels of a launch vehicle. It revealed that all natural frequencies of the system are significantly above the critical range of launcher-induced excitation (20 to 120 Hz), as required by the Cal Poly CubeSat Design Specification (CDS Rev. 14) and NASA GEVS (General Environmental Verification Standard) standards, which recommend a minimum fundamental frequency greater than 100 Hz. This ensures non-coupling with the launcher's vibration modes, mitigating the risk of resonance

during orbital transport.

Furthermore, the comparison between the simulated normal stresses and the allowable stress of 6061-T6 aluminum demonstrates largely safe margins. The most stressed region of the structure exhibits a maximum stress of 101 MPa, a value lower than the estimated allowable stress of 276 MPa.

Therefore, the results confirm that the CubeSat fully meets the structural integrity and dynamic performance criteria required for safe and successful integration into a P-POD-based launch system. The careful application of technical standards and good design practices ensures the reliability of the structure and directly contributes to the success of the space mission.

Thanks to structural damping ($\xi = 2\%$), the resonant response was smoothed, and no natural frequency coincided directly with the critical excitation zone. This significantly reduces the risk of resonant amplification and contributes to the safety of the overall design, as damping reduces the intensity of the response in resonant modes.

All normal stresses are well below the allowable stress. This indicates that, even in situations with the highest vibrational excitation (such as a P-POD launch), the CubeSat's structural integrity is maintained with a wide safety margin.

Finally, it is noted that fatigue failure is preserved for the loading levels expected in a standard launch (10^3–10^5 cycles).

The total harmonic response shows stable and controlled behavior, indicating that even in the case of excitations close to natural frequencies, the structure will not exhibit dangerous displacement amplification. This validates the robustness of the design and the safety of the structure during launch.

This analysis reinforces the conclusion that the CubeSat is structurally safe and dynamically stable for launch via P-POD, meeting the requirements of Cal Poly [02], NASA GEVS, and other aerospace engineering best practices.

The simulation results confirm that the CubeSat meets all structural and dynamic performance requirements established by Cal Poly CDS and NASA GEVS. The combination of modal analysis, harmonic response with damping ($\xi = 2\%$), stress comparison, and fatigue evaluation demonstrates the system's robustness under launcher conditions. Therefore, the CubeSat is considered safe, reliable, and mission-ready for deployment via P-POD systems.

Acknowledgments. The authors confirm that they are solely responsible for the authorship of this work and that all material included here as part of this article is the property (and authorship) of the authors or has the permission of the owners to be included here.

Declaration of authorship. The authors confirm that they are solely responsible for the authorship of this work and that all material included here as part of this article is the property (and authorship) of the authors or has the permission of the owners to be included here.

References

[01] Furger, S. *ANALYSIS AND MITIGATION OF THE CUBESAT DYNAMIC ENVIRONMENT*, 2013 (in English).
[02] *CubeSat Design Specification Rev. 14.1 The CubeSat Program, Cal Poly SLO CubeSat Design Specification Cal Poly-San Luis Obispo, CA Document Classification X Public Domain*, 2022 (in English).
[03] *QB50 System Requirements and Recommendations Issue 7*, 2015 (in English).
[04] Rivera, P. *DYNAMIC RESPONSE VALIDATION OF CUBESATS THROUGH TESTING AND FINITE ELEMENT ANALYSIS*, 2019 (in English).
[05] C. E. N. Mazzilli, J. C. André, M. L. Bucalem, S. Cifú. Lições em Mecânica das Estruturas. Blucher, 2016 (in Portuguese).
[06] R. M. Brasil and M. A. Silva, Introdução à dinâmica das estruturas. 2.ª ed. Blucher, São Paulo, 2015 (in Portuguese).
[07] R. M. Brasil and M. A. Silva, Otimização de Projetos de Engenharia. Blucher, São Paulo, 2019 (in Portuguese).
[08] T. Belytschko. *A first course in Blab La Blab*. Publisher, 2021 (in English).

[09] T. J. R. Hughes. Structural Modeling of *Blab La Blab*. PhD thesis, University of Somewhere, 2021 (in English).
[10] ASTM International, "ASTM C39/C39M-20, Standard Test Method for Compressive Strength of Cylindrical Concrete Specimens," ASTM International, 2020 (in English).
[11] Barsoum, G. I., Ibrahim, H. H., & Fawzy, M. A. Static and Random Vibration Analyses of a University CubeSat Project. *Journal of Physics: Conference Series*, *1264*. 2019 (in English).
[12] Alhammadi, A. N., Jarrar, F., Al-Shaibah, M., Almesmari, A., Vu, T., Tsoupos, A., & Marpu, P. Effect of finite element model details in structural analysis of CubeSats. CEAS Space Journal, 13(2), 231–246, 2021 (in English).
[13] Martha, L. F. Análise de Estruturas: Conceitos e Métodos Básicos, 3ª Edição. 3. ed. Rio de Janeiro: Grupo GEN, 2022 (In Portuguese).
[14] H. Yserentant, A short theory of the Rayleigh–Ritz Method. Computational Methods in Applied Mathematics, v. 13, n. 4, p. 495-502, 2013 (in English).
[15] Salem, A., Tawfik, A., Saleh, E., & Ibrahim, H. (2020). Optimum structural design of a cubesat subjected to launcher mechanical environment. Proceedings of the International Conference on Structural Dynamic , EURODYN, 2, , 2020 (In English).